Published in final edited form as:
*Radiat Res*. 2012 April ; 177(4): 365–375.

# Application of Optical Imaging and Spectroscopy to Radiation Biology

**Gregory M. Palmer**[a,1], **Karthik Vishwanath**[b], and **Mark W. Dewhirst**[a,b]

[a]Department of Radiation Oncology, Duke University Medical Center

[b]Department of Biomedical Engineering, Duke University, Durham, North Carolina 27708

## Abstract

Optical imaging and spectroscopy is a diverse field that has been of critical importance in a wide range of areas in radiation research. It is capable of spanning a wide range of spatial and temporal scales, and has the sensitivity and specificity needed for molecular and functional imaging. This review will describe the basic principles of optical imaging and spectroscopy, highlighting a few relevant applications to radiation research.

## INTRODUCTION

Optical imaging and spectroscopy is a highly diverse and active field throughout the sciences, including radiation research. Here we provide an overview of some of the basic principles underlying many of the more widely employed optical methods and, in particular, quantitative approaches that are currently being applied to the field of radiation research. This review will focus on physiological assessment of tumors prior to and after radiation therapy, and will not discuss therapeutic applications of light, such as photothermal therapy (1, 2), low-level light therapy (3, 4), and photodynamic therapy (5, 6), which could be complementary to radiation therapy. There are several potential applications of optical imaging and spectroscopy to radiation therapy, most notable the potential for pretreatment assessment of tissue hypoxia and other physiological parameters, real-time monitoring of treatment response, and basic science studies investigating molecular responses to radiation therapy. Advantages of optical methods include their high specificity and sensitivity, with a wide range of functional endpoints possible. In addition, they utilize nonionizing radiation, providing a relatively safe imaging modality that does not increase overall ionizing radiation exposure to patients. Finally, they are also generally much lower in cost compared to other imaging methods, and combined with their overall safety, this makes them highly suitable for repeated measurements. There are also some fundamental limitations in the clinical applicability of optical methods, including the relatively high scattering in tissue at optical and near-infrared wavelengths, which limits resolution and penetration depth compared to X ray and other imaging modalities. This review will highlight the use of optical methods for studying radiation therapy and response, and their potential utility in clinical applications.

Several clinically relevant aspects of radiation biology are amenable to study by optical sensing as an investigative tool; for example, there is a strong dependence on oxygen for the efficacy of radiation therapy, with hypoxic tumors being up to three times more resistant to radiation therapy (7). In addition, re-oxygenation, the phenomenon whereby hypoxic cells



[1]Address for correspondence: Duke University Medical Center, Radiation Oncology, Box 3455, Durham, NC 27710; greg.palmer@duke.edu. .

re-oxygenate as multiple fractions of radiation and are delivered to a tumor, is the primary mechanism by which hypoxic tumors can be treated clinically, and is also the basis for fractionated dosing schedules (7). Since many optical techniques are innately sensitive to tissue oxygenation due to the strong intrinsic absorption of oxygen by hemoglobin, optical techniques are potentially useful for predicting and monitoring the response to therapy.

Secondly, negative side effects of normal tissue radiation exposure can potentially be monitored by optical methods. For example, Muanza *et al.* (8) and Kawakami-Wong *et al.* (9) have investigated the use of OCT based imaging to score oral mucositis. In this case, the method is sensitive to the changes in tissue morphology as a consequence of the development of mucositis.

Finally, as a preclinical tool, optical sensing has distinct advantages due to the wide range of functional probes and reporters available to provide insight into the molecular responses of tissues to radiation therapy.

## Optical Measurement Modalities

Optical sensing is a broad field, with many different technologies that may be applied to different problems, including traditional imaging methods such as fluorescence and reflectance microscopy and wide field imaging, and newer approaches including optical coherence tomography(10) and photoacoustic tomography (11). These methods can be broadly categorized as measuring either ballistic or diffusely scattered photons. Ballistic, or unscattered photons, enable high-resolution imaging but limited penetration depth (e.g., as with traditional microscopy), whereas diffusely scattered photons can be detected with a much deeper penetration depth, but afford more limited resolution. A hybrid method is photoacoustic tomography (PAT), which uses diffuse photons to initiate an acoustic signal, which can then be detected as a ballistic wave, combining deep penetration with high resolution. A brief overview of the sources of contrast and broad categories of widely available technologies that are covered in this review are listed in Tables 1 and 2, respectively.

## Optical Properties

*In vivo* optical methods in general rely on the ability to couple light into and out of tissue and quantify the interaction of light within the tissue in some manner. As a result, all of these methods are sensitive to the characteristics of light propagation in tissue; notably refraction, reflection, scattering, and absorption (21). The first three of these arise from mismatches in the refractive index of light, as between air and tissue, or cytoplasm and lipid bilayers, and serve to alter the direction of propagation of light. Scattering is largely a result of small subcellular or extracellular inhomogeneities in refractive index such as cellular organelles or collagen fibrils. It is wavelength-dependent, generally decreasing with increasing wavelength, and is rather high in tissue relative to other modalities, on the order of 10s of interactions per mm of photon transit. The consequence is that ballistic photons (i.., photons that traverse tissue without encountering any scattering events) can only effectively penetrate into the superficial layers of tissue (hundreds of micrometers). Deeper than this, the majority of photons are multiply scattered, or diffuse, and spatial resolution is greatly diminished. It is this feature of tissue optical properties that limits ballistic imaging depth (as in confocal or multiphoton microscopy). The alternative is to detect diffusely-scattered photons, which carry information from deeper within the tissues, but at the cost of greatly diminished image resolution (on the order of 1 mm to 1 cm).

Absorption of light in tissue also plays a significant role in the transmission of optical signals through tissue. It also generally decreases with wavelength, but is highly tissue-

specific. Ultraviolet (UV) absorption is high due to the presence of strongly UV-absorbing biological chromophores. Visible wavelength absorption is dominated by hemoglobin in most tissues, and is thus dependent on the vascularity and oxygenation of the tissue. Hemoglobin absorption drops significantly at wavelengths longer than 650 nm, as seen in Fig. 1. This enables deeper penetration of these longer wavelengths of light into tissue. Water absorption becomes significant above approximately 900 nm, and increases into the infrared. This region of relatively low tissue absorption is referred to as the NIR window, and has been exploited to enable relatively deep tissue imaging using diffusely-scattered light.

Fluorescence is another fundamental interaction of light with matter that is commonly exploited for optical imaging. Physically, fluorescence occurs when an electron orbiting a fluorophore absorbs a photon, promoting it to an excited state. While in the excited state, the electron will relax down to the lowest vibration energy level in the excited state, releasing some energy as heat. After some amount of time (typically on the order of nanoseconds), the electron will decay back to the lower energy state, releasing a photon. The energy lost due to relaxation is reflected in the longer wavelength of the emitted photon compared to the absorbed photon, which is referred to as the Stokes shift. Because a given fluorophore has characteristic absorption and emission spectra, it is possible to use several fluorophores of different wavelengths to probe different aspects of a sample's properties.

Finally, bioluminescence is commonly employed in small animal research using transgenic animals or cells transfected with luciferase genes. The luciferase protein generates a photon in the presence of its particular substrate(s), which are commonly injected prior to imaging. This provides a means of monitoring gene expression, cell tracking, or other phenomena similar to what is possible with fluorescence proteins. The primary difference is there is no need for excitation light to produce an emitted photon, which leads to much lower background signals and better sensitivity.

Because tissue absorption and scattering properties play such a fundamental role in the measurement of optical signals from tissue, it is crucial to recognize and account for their importance in developing any quantitative measure of optical signals. Small animal imaging is one example. For a bioluminescence or fluorescence source, attenuation will play a significant role in determining the magnitude of the signal collected; deeper sources will appear significantly dimmer or may not be visible at all at the detector.

## Intrinsic Optical Contrast

The intrinsic tissue optical properties including scattering, absorption, and fluorescence (autofluorescence) can be confounding factors in many applications, but they may also be exploited as sources of contrast. Because absorption has a strong dependence on both the total amount of hemoglobin as well as its oxygenation state, this has served as an intrinsic marker of tissue hypoxia and vascularity (12). Tissue autofluorescence arises from a range of fluorophores, notably collagen, elastin, tryptophan, and the electron carriers NADH and FAD (12). NADH and FAD are particularly interesting because their redox pairs, NAD and $FADH_2$ are nonfluorescent. Thus, autofluorescence from NADH and FAD can be exploited to quantify the cellular redox ratio (25, 26). Finally, tissue scattering is dependent on tissue morphology, and thus can be used to distinguish different tissue types, such as breast parenchyma and adipose (27), or necrosis and viable tissue (28).

## Molecular, Morphological, and Functional Imaging Probes and Reporters

Exogenous fluorophores and fluorescent reporter genes are capable of reporting a wide range of parameters such as nuclear, mitochondrial, extracellular-matrix localization, or

tissue oxygen tension (29–31), reactive oxygen/nitrogen species (32, 33), and apoptosis (34). A number of excellent resources are available describing the wide range of parameters that can be investigated using current techniques (20, 35–42). There are several approaches commonly employed, and these can be broadly categorized by probes whose localization is of interest, and probes whose properties are altered by the functional parameter of interest.

The simplest localization probes are nonspecific probes or nanoparticles. Probes of differing sizes have been used to study vascular perfusion and permeability (43, 44). A probe may also be targeted to a specific receptor, transporter, or other entity by its chemical structure or through conjugation to other molecules or ligands. These are no different from imaging agents that could be used with other modalities, except that they are conjugated to a fluorophore. For example, fluorescent probes conjugated to antibodies have been used to monitor vascular endothelial growth factor (VEGF) expression (45). Gold nanoparticles have similarly been used as scattering contrast for identifying epidermal growth factor expression in precancers (46).

Functional probes can be constructed to alter their properties based on the local environment. These include lifetime-based sensors for oxygen tension, ratiometric reporters, and many pH probes (20). These probes change their fluorescence intensity, decay rate, or emission spectrum based on their local environments. Additionally, a fluorophore can also be conjugated to a quencher via a linker that is cleaved by a specific enzyme, which enables probing of specific enzymatic activity (42, 47).

Genetic reporters are widely used to study gene expression and interactions, as well as functional reporters, e.g., for calcium-ion concentration (48). Green fluorescence protein (GFP) is the classic example (49), but this has extended to a wide range of available colors, and into the NIR (50, 51), to facilitate whole animal imaging. Finally, bioluminescence is another mechanism commonly exploited for *in vivo* imaging. These methods require a genetic reporter, such as the firefly luciferase, which operates by converting chemical energy into light. Firefly luciferase (often abbreviated *luc*) is a commonly used variety and converts luciferin (an injectable substrate), oxygen, and ATP into light in a two-step process, with emission that is primarily in the yellow-green spectrum (52).

## APPLIED TECHNOLOGIES

### Fiber Optic-Based Tissue Spectroscopy

Fiber optic sensors offer a relatively simple system for carrying out quantitative spectroscopy of tissue. They typically involve illuminating and collecting light spectra from tissue via a fiber optic probe that couples a broadband light source and spectrometer detector to the site of interest. Specific wavelength filters, or monochromators, enable selection of excitation and collection wavelengths, and allow collection of either tissue fluorescence spectra or the diffusely reflected light spectra (commonly referred to as light-scattering spectroscopy or diffuse-reflectance spectroscopy). These measurements can then be analyzed to extract the wavelength-dependent intrinsic absorption, scattering, and fluorescence properties of the tissue. Quantitative models of light tissue interaction based on Monte Carlo methods or analytical approximations are used to extract these underlying optical properties (12, 21), which in turn provide information about the intrinsic sources of contrast described above, and/or any exogenous contrast agents that may be in use. Alternatively, empirical and statistical approaches have been used to classify tissues directly from the measured reflectance or fluorescence spectra, but have limited ability to provide insight about the mechanistic or physical characteristics of the tissues (53, 54).

These types of approaches have been applied to a wide range of biological problems, ranging from cancer diagnosis and margin assessment to evaluation of therapeutic response, including radiotherapy (12, 55–57). As a recent example, Vishwanath *et al.* investigated the ability of optical spectroscopy to predict for local tumor control after radiation therapy in a preclinical study (57). They irradiated a head and neck xenograft with a 50% tumor control dose ($TCD_{50}$, the dose at which 50% of animals will have local control), and found that early changes in vascular hemoglobin oxygen saturation were statistically different in animals that showed a local control after therapy relative to those that had tumor regrowth, and that these effects preceded differences in tumor volume, as shown in Fig. 2.

## Intravital Microscopy

Another commonly used tool is intravital microscopy. This involves either placing a small animal on a conventional microscope, or imaging the subject using a portable endoscopic or hand-held microscope. The technique relies on the detection of focused, unscattered light. Because of the limited penetration depth of ballistic photons, this is restricted to superficial or endoscopically-accessible sites (58, 59), or requires the implantation of a window chamber into the subject (60). The use of high-resolution microscopy techniques including wide-field fluorescence, transmitted or reflected light imaging, confocal, and multiphoton microscopy enables characterization of a wide range of morphological and functional features. For example, a wide range of hemodynamic parameters can be obtained including microvascular network geometry (60), red cell flux (61), microvascular hemoglobin oxygen saturation (62), and vascular permeability (60). These methods are describe in detail in a recent protocols paper (63), and an example of the resulting functional and morphological data obtainable are shown in Fig. 3. These can often be combined with exogenous fluorophores and fluorescent reporter genes capable of reporting a wide range of parameters as described above.

As an example, Moeller *et al.* demonstrated the induction of HIF-1 after irradiation using a GFP-based fluorescence reporter of HIF-1 activity (32). They found that tumor reoxygenation following radiotherapy leads to increased HIF-1 activity due to the presence of reactive oxygen species. An increase in HIF-1-regulated proteins furthermore resulted from the accumulation and release of stress granules. It has since been shown that HIF-1 activation is protective of endothelial cells after radiation, and also plays a role in regeneration of the vascular network by vasculogenesis (64–67). To provide an additional example, Cummings *et al.* monitored the migration of dendritic cells in the ear epithelium following ionizing radiation using confocal imaging (68). They reported a significant decrease in the density of MHC class II positive cells after local irradiation, and that administration of interleukin-12 significantly reduced migration of these cells from the site of irradiation.

Another approach with more direct clinical relevance is intravital imaging techniques suitable for endoscopic or intraoperative imaging, including commercially available microendoscopy systems (39, 58, 69–79). High-resolution confocal microendoscopy has particular potential as a diagnostic, prognostic, and monitoring tool that is capable of monitoring cellular level morphology suitable for *in vivo* pathology (58). Both reflectance- and fluorescence-based systems have been described, and are therefore amenable to any of the contrast agents described in this review.

## Diffuse Optical Imaging and Tomography

Another class of technologies involves the use of diffusely-scattered photons for imaging and includes a family of techniques that can be broadly separated into tomographic and planar imaging methods. This includes diffusely-scattered transmission, reflectance, and

fluorescence, and therefore is capable of quantifying all three of these parameters. Tomographic methods in general require a solution of the light transport equation to extract the optical properties in three dimensions. This is an difficult problem, and a variety of methods have been developed both in terms of hardware and data analysis for a range of length scales from sub-millimeters up to several centimeters of penetration (17, 21, 80–85). A comprehensive review of these methods and techniques will not be attempted here. The ultimate goal of these techniques is to quantitatively extract the tissue absorption, scattering, and/or fluorescence properties at each voxel of a predefined 3-dimensional (3D) mesh. Fluorescence molecular tomography (FMT) is one such application that has become relatively widely adopted and commercialized, which provides the 3D reconstruction fluorophore concentration within a small animal (18).

Commonly, imaging is done using planar, 2D imaging systems, particularly in small animal imaging systems. These typically illuminate the entire field of view with a laser (or filtered white light source) and collect the emitted fluorescent light via a camera. An example of both types of techniques is shown if Fig. 4. Kirsch *et al.* investigated the ability of an NIR probe for protease activity to identify tumor margins during a surgical procedure in a novel sarcoma model (86). Soft tissue sarcomas are commonly treated with radiation followed by surgical resection, so the ability to remove the entire tumor is critical to effective treatment. Of relevance to this review is the use of a commercial FMT system (FMT, VisEn Medical Inc.) to quantify the concentration of activated probe within the tumor (Fig. 4c, d), as well as a hand-held planar imaging device (HHD, Siemens) to image the resection cavity after surgical excision of the tumor mass (Fig. 4e).

## Optical Coherence Tomography

Optical coherence tomography (OCT) is an interferometric technique that probes the coherent backscattering of light from tissue and is often referred to as the optical equivalent of ultrasound (10). In its simplest form it is set up as a Michelson interferometer. Low coherence, broadband light is coupled to the tissue via the sample arm, and interference patterns between the reflected tissue signal and the reference arm provides the OCT signal. The depth of the measured interference pattern is tuned for different depths within tissue by changing the path-length of the reference arm to provide a 1D depth scan (also referred to as an A-scan) (21). Two-dimensional or 3D reconstructions are obtained by raster scanning the source on the tissue surface along a line or surface. The contrast obtained via the interference spectrum in OCT emerges from spatial variations in optical scattering and/or refractive indices of the tissue and, thus, OCT is very valuable as a technique to image histological/morphological/architectural features of tissue microstructure. Since the depth of penetration of light in tissue depends on the optical absorption and scattering properties of the tissue, which typically are lower in the NIR spectral region (relative the visible/UV regions), OCT sources typically use wavelengths spanning between 650–900 nm. With these wavelengths, the sensing depth of OCT systems ranges from 1 to 3 mm. Axial and lateral resolutions of typical OCT systems range between 1 to 10 μm and 10 to 50 μm, respectively. A vast majority of clinical applications using OCT have measured disorders and irregularities in human eyes including the microstructure of cornea, retinopathy, macular degeneration, and subretinal neovascularization. Besides the eye, other clinical applications include the detection of vulnerable plaques in atherosclerosis, where images of arteries are obtained via catheter-based OCT methods to distinguish calcium deposits, plaques and calcification. In cancer applications, the predominant use of OCT is focused around early diagnosis of precancerous lesions in gastroenterology, pulmonary medicine and skin lesions.

There are fewer reports indicating the utility of OCT for radiation research. Studies by Muanza *et al.* (8) and Kawakami-Wong *et al.* (9) have investigated the use of OCT-based imaging in preclinical and clinical studies to score oral mucositis in subjects receiving

radiation and/or chemotherapy, and showed that OCT-based sensing was able to detect occurrence of mucositis earlier than other typically used visual scoring. More recent developments in functional OCT based imaging to detect vascularization (via spectral OCT) and blood flow (by Doppler OCT) have also shown significant impact for applications in radiation research. Doppler OCT has also been used by several studies to detect changes in vascular flow and hemodynamics following tumor treatment with radiation, vascular disrupting agents, and photodynamic therapy (87–91). Such reports highlight the applicability of OCT-based imaging in radiation research.

## Photoacoustic Tomography

As a final technology, we discuss the photoacoustic method implemented as photoacoustic tomography (PAT), which is seeing a tremendous amount of activity in recent years (11). This method relies on the photoacoustic effect, whereby an exciting (ultra-short) light pulse is absorbed by chromophores in the tissue of interest (such as hemoglobin, water, or fat naturally present in the tissue, or by micro-bubbles or nanoparticles introduced as contrast agents). This absorption process induces a rapid thermal expansion in the tissue and causes the emission of a broadband ultrasound pressure wave, which is then detected using regular ultrasonic transducers placed around the tissue. This method combines the advantages of having optical sources of contrast (due to the optical nature of light-tissue interactions) with the depth sensitivity of ultrasound (due to the propagation of ultrasound in tissue), along with the deep tissue (11). Photoacoustic methods offer 3D tomographic reconstructions of tissue and use one of two approaches: a large array of transducers to simultaneously sense the emitted ultrasonic signals from the absorption of the light, and then subsequently reconstruct the sources of the emitted signals via inverse methods; or by using a single transducer element that is raster-scanned across the tissue surface to form a 3D map by using a depth-scan at each point on the tissue surface to directly reconstruct the emitted photoacoustic signal from the tissue. These methods are called PACT (photoacoustic computed tomography) and PAM (photoacoustic microscopy), respectively (92). PACT-based 3D reconstruction methods are computationally intensive, require complex instrumentation, but provide very high frame rates for imaging. On the other hand, PAM is much simpler in terms of image reconstruction and instrumentation, but is slow in terms of imaging a given volume of tissue since there is a need to raster scan the whole surface of interest.

Given that the absorption contrast relied upon by photoacoustic tomography emerges naturally from blood, a major absorber of light in tissues, PAT has been extensively used in clinical and preclinical studies to image subsurface vasculature in applications ranging from neuro-imaging, sensing vascular remodeling (after ischemia or injury), and tumor imaging (93–96). Further, given the advent of functionalized gold and carbon nanoparticles as molecularly-targeted contrast agents, and the fact that these nanoparticles present extremely high absorption cross-sections, they are being actively researched for use in conjunction with PAT methods (97–101). Although there are no available reports at the current time reporting on the use of PAT in the field of radiation research, a recent report highlights the applicability of using PAT methods to monitor tumor biochemistry and molecular changes in transgenic animal models, as seen in Fig. 5 (102). Here, the authors used PAT to quantify the changes in capillary morphogenesis, vascular remodeling, and microvessel regression in an animal model that constitutively expressed oxygen independent HIF-1 in the skin, even during persistent activation of VEGFR-2. Such studies demonstrate the promise of PAT-based longitudinal sensing to quantify the impact of radiation, chemotherapy, and molecular therapies across treatment regimes.

## CONCLUSIONS

In summary, optical imaging and spectroscopy is a diverse field encompassing a wide array of technologies and applications. The key advantage of these techniques is that they are able to elucidate the spatiotemporal dynamics of the therapeutic response. Arbitrary selection of one or two time points for histology or other imaging modality such as PET may miss the event in question. This advantage must be balanced against the relatively limited sensing depth and potential perturbation of the system by window chamber implantation (if required).Incorporation of these techniques into radiobiological investigation enables insight into virtually every aspect of radiobiology. As technology develops, we can expect that sensitivity, resolution, and molecular specificity will continue to improve, and that more of these approaches will be translated to the clinic.

## Acknowledgments

This work was supported by the National Institutes of Health (MWD: R01CA40355 and KVH: 5K99CA140783-02).

## REFERENCES

1. Kennedy LC, Bickford LR, Lewinski NA, Coughlin AJ, Hu Y, Day ES, et al. A New Era for Cancer Treatment: Gold-Nanoparticle-Mediated Thermal Therapies. Small. 2011; 7(2):169–83. [PubMed: 21213377]
2. Stafford RJ, Fuentes D, Elliott AA, Weinberg JS, Ahrar K. Laser-Induced Thermal Therapy for Tumor Ablation. Critical Reviews in Biomedical Engineering. 2010; 38(1):79–100. [PubMed: 21175405]
3. Hashmi JT, Huang Y-Y, Sharma SK, Kurup DB, De Taboada L, Carroll JD, et al. Effect of Pulsing in Low-Level Light Therapy. Lasers in Surgery and Medicine. 2010; 42(6):450–66. [PubMed: 20662021]
4. Peplow PV, Chung TY, Baxter GD. Laser Photobiomodulation of Proliferation of Cells in Culture: A Review of Human and Animal Studies. Photomedicine and Laser Surgery. 2010; 28:S3–S40. [PubMed: 20666617]
5. Wilson BC, Patterson MS. The physics, biophysics and technology of photodynamic therapy. Physics in Medicine and Biology. 2008; 53(9):R61–R109. [PubMed: 18401068]
6. Celli JP, Spring BQ, Rizvi I, Evans CL, Samkoe KS, Verma S, et al. Imaging and Photodynamic Therapy: Mechanisms, Monitor-ing, and Optimization. Chemical Reviews. 2010; 110(5):2795–838. [PubMed: 20353192]
7. Hall, EJ.; Giaccia, AJ. Radiobiology for the radiologist. 6th ed. Vol. ix. Lippincott Williams & Wilkins; Philadelphia: 2006. p. 546
8. Muanza TM, Cotrim AP, McAuliffe M, Sowers AL, Baum BJ, Cook JA, et al. Evaluation of radiation-induced oral mucositis by optical coherence tomography. Clin Cancer Res. 2005; 11(14): 5121–7. Epub 2005/07/22. [PubMed: 16033826]
9. Kawakami-Wong H, Gu S, Hammer-Wilson MJ, Epstein JB, Chen Z, Wilder-Smith P. In vivo optical coherence tomography-based scoring of oral mucositis in human subjects: a pilot study. J Biomed Opt. 2007; 12(5) doi:051702. Epub 2007/11/13.
10. Huang D, Swanson EA, Lin CP, Schuman JS, Stinson WG, Chang W, et al. Optical coherence tomography. Science. 1991; 254(5035):1178–81. Epub 1991/11/22. [PubMed: 1957169]
11. Wang L. Multiscale photoacoustic microscopy and computed tomography. Nat Photonics. 2009; 3(9):503–9. [PubMed: 20161535]
12. Brown JQ, Vishwanath K, Palmer GM, Ramanujam N. Advances in quantitative UV-visible spectroscopy for clinical and pre-clinical application in cancer. Curr Opin Biotechnol. 2009; 20(1): 119–31. Epub 2009/03/10. [PubMed: 19268567]

13. Tuchin, VV.; Society of Photo-optical Instrumentation Engineers. Tissue optics: light scattering methods and instruments for medical diagnosis. 2nd ed. Vol. xl. SPIE/International Society for Optical Engineering; Bellingham, Wash.: 2007. p. 840
14. Ramanujam, N. Fluorescence Spectroscopy In Vivo. In: Meyers, R., editor. Encyclopedia of Analytical Chemistry. John Wiley and Sons, Ltd.; 2000. p. 20-56.
15. Prasad, PN. Introduction to biophotonics. Vol. xvii. Wiley-Interscience; Hoboken, NJ: 2003. p. 593p. 8of plates p
16. Xu M, Wang L. Photoacoustic imaging in biomedicine. Review of Scientific Instruments. 2006; 77(4)
17. Gibson AP, Hebden JC, Arridge SR. Recent advances in diffuse optical imaging. Phys Med Biol. 2005; 50(4):R1–43. [PubMed: 15773619]
18. Ntziachristos V, Ripoll J, Wang LV, Weissleder R. Looking and listening to light: the evolution of whole-body photonic imaging. Nat Biotechnol. 2005; 23(3):313–20. [PubMed: 15765087]
19. Mycek, M-A.; Pogue, BW. Handbook of biomedical fluorescence. Vol. xv. Marcel Dekker; New York: 2003. p. 665
20. Weissleder, R. Molecular imaging: principles and practice. People's Medical Pub. House; Shelton, CT: 2009.
21. Wang, LV.; Wu, H-i. Biomedical optics: principles and imaging. Vol. xiv. Wiley-Interscience; Hoboken, NJ: 2007. p. 362
22. Prahl, S. Optical absorption of hemoglobin Oregon Medical Laser Center. 2008. [cited 2008]; Available from: http://omlc.ogi.edu/spectra/hemoglobin
23. Segelstein, D. The complex refractive index of water. University of Missouri; Kansas City, MO: 1981.
24. Palmer, GM.; Vishwanath, K. In vivo fluorescence imaging and spectroscopy. In: Splinter, R., editor. Handbook of physics in medicine and biology. CRC Press/Taylor & Francis Group; Boca Raton, FL: 2010. p. 30-1-11.
25. Chance B, Schoener B, Oshino R, Itshak F, Nakase Y. Oxidation-reduction ratio studies of mitochondria in freeze-trapped samples. NADH and flavoprotein fluorescence signals. J Biol Chem. 1979; 254(11):4764–71. [PubMed: 220260]
26. Chance B, Nioka S, Warren W, Yurtsever G. Mitochondrial NADH as the bellwether of tissue O2 delivery. Adv Exp Med Biol. 2005; 566:231–42. Epub 2006/04/06. [PubMed: 16594157]
27. Palmer G, Zhu C, Breslin T, Xu F, Gilchrist K, Ramanujam N. Monte Carlo-based inverse model for calculating tissue optical properties. Part II: Application to breast cancer diagnosis. Appl Opt. 2006; 45(5):1072–8. Epub 2006/03/04. [PubMed: 16512551]
28. Vishwanath K, Yuan H, Barry W, Dewhirst M, Ramanujam N. Using optical spectroscopy to longitudinally monitor physiological changes within solid tumors. Neoplasia. 2009; 11(9):889–900. [PubMed: 19724683]
29. Zhang G, Palmer G, Dewhirst M, Fraser C. A dual-emissive-materials design concept enables tumour hypoxia imaging. Nat Mater. 2009; 8(9):747–51. [PubMed: 19668206]
30. Palmer GM, Fontanella AN, Zhang G, Hanna G, Fraser CL, Dewhirst MW. Optical imaging of tumor hypoxia dynamics. J Biomed Opt. 2010 In press.
31. Càrdenas-Navia LI, Mace D, Richardson RA, Wilson DF, Shan S, Dewhirst MW. The pervasive presence of fluctuating oxygenation in tumors. Cancer Res. 2008; 68(14):5812–9. [PubMed: 18632635]
32. Moeller BJ, Cao Y, Li CY, Dewhirst MW. Radiation activates HIF-1 to regulate vascular radiosensitivity in tumors: role of reoxygenation, free radicals, and stress granules. Cancer Cell. 2004; 5(5):429–41. Epub 2004/05/18. [PubMed: 15144951]
33. Fukumura D, Duda DG, Munn LL, Jain RK. Tumor Microvasculature and Microenvironment: Novel Insights Through Intravital Imaging in Pre-Clinical Models. Microcirculation. 2010; 17(3): 206–25. [PubMed: 20374484]
34. Niu G, Chen XY. Apoptosis Imaging: Beyond Annexin V. Journal of Nuclear Medicine. 2010; 51(11):1659–62. [PubMed: 20956479]

35. Hof, M.; Hutterer, R.; Fidler, V. Fluorescence spectroscopy in biology: advanced methods and their applications to membranes, proteins, DNA, and cells. Vol. xix. Springer; Berlin; New York: 2005. p. 305
36. Prasad, PN. Introduction to biophotonics. Vol. xvii. Wiley-Interscience; Hoboken, NJ: 2003. p. 593p. 8of plates p
37. Lakowicz, JR. Principles of fluorescence spectroscopy. 3rd ed. Vol. xxvi. Springer; New York: 2006. p. 954
38. Thompson, RB. Fluorescence sensors and biosensors. CRC/Taylor & Francis; Boca Raton: 2006. p. 395
39. Pierce MC, Javier DJ, Richards-Kortum R. Optical contrast agents and imaging systems for detection and diagnosis of cancer. Int J Cancer. 2008; 123(9):1979–90. Epub 2008/08/21. [PubMed: 18712733]
40. Massoud TF, Gambhir SS. Integrating noninvasive molecular imaging into molecular medicine: an evolving paradigm. Trends Mol Med. 2007; 13(5):183–91. Epub 2007/04/04. [PubMed: 17403616]
41. Ntziachristos V, Bremer C, Weissleder R. Fluorescence imaging with near-infrared light: new technological advances that enable in vivo molecular imaging. European Radiology. 2003; 13(1): 195–208. [PubMed: 12541130]
42. Weissleder R, Pittet MJ. Imaging in the era of molecular oncology. Nature. 2008; 452(7187):580–9. [PubMed: 18385732]
43. Dreher MR, Liu W, Michelich CR, Dewhirst MW, Yuan F, Chilkoti A. Tumor vascular permeability, accumulation, and penetration of macromolecular drug carriers. J Natl Cancer Inst. 2006; 98(5):335–44. Epub 2006/03/02. [PubMed: 16507830]
44. Yuan F, Dellian M, Fukumura D, Leunig M, Berk DA, Torchilin VP, et al. Vascular permeability in a human tumor xenograft: molecular size dependence and cutoff size. Cancer Res. 1995; 55(17): 3752–6. [PubMed: 7641188]
45. Chang SK, Rizvi I, Solban N, Hasan T. In vivo optical molecular imaging of vascular endothelial growth factor for monitoring cancer treatment. Clin Cancer Res. 2008; 14(13):4146–53. [PubMed: 18593993]
46. Sokolov K, Follen M, Aaron J, Pavlova I, Malpica A, Lotan R, et al. Real-time vital optical imaging of precancer using anti-epidermal growth factor receptor antibodies conjugated to gold nanoparticles. Cancer Res. 2003; 63(9):1999–2004. [PubMed: 12727808]
47. Bremer C, Tung CH, Weissleder R. In vivo molecular target assessment of matrix metalloproteinase inhibition. Nat Med. 2001; 7(6):743–8. [PubMed: 11385514]
48. Miyawaki A, Llopis J, Heim R, McCaffery JM, Adams JA, Ikura M, et al. Fluorescent indicators for Ca2+based on green fluorescent proteins and calmodulin. Nature. 1997; 388(6645):882–7. [PubMed: 9278050]
49. Tsien RY. The green fluorescent protein. Annu Rev Biochem. 1998; 67:509–44. Epub 1998/10/06. [PubMed: 9759496]
50. Shcherbo D, Shemiakina II, Ryabova AV, Luker KE, Schmidt BT, Souslova EA, et al. Near-infrared fluorescent proteins. Nat Methods. 2010; 7(10):827–9. [PubMed: 20818379]
51. Shu X, Royant A, Lin MZ, Aguilera TA, Lev-Ram V, Steinbach PA, et al. Mammalian expression of infrared fluorescent proteins engineered from a bacterial phytochrome. Science. 2009; 324(5928):804–7. [PubMed: 19423828]
52. Inouye S. Firefly luciferase: an adenylate-forming enzyme for multicatalytic functions. Cell Mol Life Sci. 2010; 67(3):387–404. [PubMed: 19859663]
53. Zhu C, Palmer GM, Breslin TM, Harter J, Ramanujam N. Diagnosis of breast cancer using diffuse reflectance spectroscopy: Comparison of a Monte Carlo versus partial least squares analysis based feature extraction technique. Lasers Surg Med. 2006; 38(7):714–24. Epub 2006/06/27. [PubMed: 16799981]
54. Skala MC, Palmer GM, Vrotsos KM, Gendron-Fitzpatrick A, Ramanujam N. Comparison of a physical model and principal component analysis for the diagnosis of epithelial neoplasias in vivo using diffuse reflectance spectroscopy. Opt Express. 2007; 15(12):7863–75. Epub 2007/10/04. [PubMed: 17912337]

55. Sunar U, Quon H, Durduran T, Zhang J, Du J, Zhou C, et al. Noninvasive diffuse optical measurement of blood flow and blood oxygenation for monitoring radiation therapy in patients with head and neck tumors: a pilot study. J Biomed Opt. 2006; 11(6):064021. [PubMed: 17212544]
56. Sunar U, Makonnen S, Zhou C, Durduran T, Yu G, Wang HW, et al. Hemodynamic responses to antivascular therapy and ionizing radiation assessed by diffuse optical spectroscopies. Opt Express. 2007; 15(23):15507–16. [PubMed: 19550836]
57. Vishwanath K, Klein D, Chang K, Schroeder T, Dewhirst M, Ramanujam N. Quantitative optical spectroscopy can identify long-term local tumor control in irradiated murine head and neck xenografts. J Biomed Opt. 2009; 14(5):054051. [PubMed: 19895152]
58. MacAulay C, Lane P, Richards-Kortum R. In vivo pathology: microendoscopy as a new endoscopic imaging modality. Gastrointest Endosc Clin N Am. 2004; 14(3):595–620. xi. [PubMed: 15261205]
59. Helmchen F, Denk W. Deep tissue two-photon microscopy. Nature Methods. 2005; 2(12):932–40. [PubMed: 16299478]
60. Huang Q, Shan S, Braun RD, Lanzen J, Anyrhambatla G, Kong G, et al. Noninvasive visualization of tumors in rodent dorsal skin window chambers. Nat Biotechnol. 1999; 17(10):1033–5. Epub 1999/10/03. [PubMed: 10504711]
61. Kimura H, Braun RD, Ong ET, Hsu R, Secomb TW, Papahadjopoulos D, et al. Fluctuations in red cell flux in tumor microvessels can lead to transient hypoxia and reoxygenation in tumor parenchyma. Cancer Res. 1996; 56(23):5522–8. Epub 1996/12/01. [PubMed: 8968110]
62. Sorg B, Moeller B, Donovan O, Cao Y, Dewhirst M. Hyper-spectral imaging of hemoglobin saturation in tumor microvasculature and tumor hypoxia development. J Biomed Opt. 2005; 10(4): 44004. Epub 2005/09/24. [PubMed: 16178638]
63. Palmer GM, Fontanella AN, Shan S, Hanna G, Zhang G, Fraser CL, et al. In vivo optical molecular imaging and analysis in mice using dorsal window chamber models applied to hypoxia, vasculature and fluorescent reporters. Nature protocols. 2011; 6(9):1355–66.
64. Kioi M, Vogel H, Schultz G, Hoffman RM, Harsh GR, Brown JM. Inhibition of vasculogenesis, but not angiogenesis, prevents the recurrence of glioblastoma after irradiation in mice. J Clin Invest. 2010; 120(3):694–705. [PubMed: 20179352]
65. Moeller BJ, Dreher MR, Rabbani ZN, Schroeder T, Cao Y, Li CY, et al. Pleiotropic effects of HIF-1 blockade on tumor radiosensitivity. Cancer Cell. 2005; 8(2):99–110. Epub 2005/08/16. [PubMed: 16098463]
66. Dewhirst MW, Cao Y, Li CY, Moeller B. Exploring the role of HIF-1 in early angiogenesis and response to radiotherapy. Radiother Oncol. 2007; 83(3):249–55. Epub 2007/06/15. [PubMed: 17560674]
67. Dewhirst M. Relationships between cycling hypoxia, HIF-1, angiogenesis and oxidative stress. Radiat Res. 2009; 172(6):653–65. [PubMed: 19929412]
68. Cummings RJ, Mitra S, Foster TH, Lord EM. Migration of skin dendritic cells in response to ionizing radiation exposure. Radiat Res. 2009; 171(6):687–97. [PubMed: 19580475]
69. Kim P, Chung E, Yamashita H, Hung K, Mizoguchi A, Kucherlapati R, et al. In vivo wide-area cellular imaging by side-view endomicroscopy. Nat Methods. 2010; 7(4):303–5. [PubMed: 20228814]
70. Sanduleanu S, Driessen A, Gomez-Garcia E, Hameeteman W, de Bruïne A, Masclee A. In vivo diagnosis and classification of colorectal neoplasia by chromoendoscopy-guided confocal laser endomicroscopy. Clin Gastroenterol Hepatol. 2010; 8(4):371–8. [PubMed: 19683597]
71. Davila R. Chromoendoscopy. Gastrointest Endosc Clin N Am. 2009; 19(2):193–208. [PubMed: 19423018]
72. Mackanos M, Hargrove J, Wolters R, Du C, Friedland S, Soetikno R, et al. Use of an endoscope-compatible probe to detect colonic dysplasia with Fourier transform infrared spectroscopy. J Biomed Opt. 2009; 14(4):044006. [PubMed: 19725718]
73. Søreide K, Nedrebø B, Reite A, Thorsen K, Kørner H. Endoscopy, morphology, morphometry and molecular markers: predicting cancer risk in colorectal adenoma. Expert Rev Mol Diagn. 2009; 9(2):125–37. [PubMed: 19298137]

74. Togashi K, Osawa H, Koinuma K, Hayashi Y, Miyata T, Sunada K, et al. A comparison of conventional endoscopy, chromoendoscopy, and the optimal-band imaging system for the differentiation of neoplastic and non-neoplastic colonic polyps. Gastrointest Endosc. 2009; 69(3 Pt 2):734–41. [PubMed: 19251019]
75. Kiesslich R, Goetz M, Vieth M, Galle P, Neurath M. Technology insight: confocal laser endoscopy for in vivo diagnosis of colorectal cancer. Nat Clin Pract Oncol. 2007; 4(8):480–90. [PubMed: 17657253]
76. Tischendorf J, Wasmuth H, Koch A, Hecker H, Trautwein C, Winograd R. Value of magnifying chromoendoscopy and narrow band imaging (NBI) in classifying colorectal polyps: a prospective controlled study. Endoscopy. 2007; 39(12):1092–6. [PubMed: 18072061]
77. Gmitro AF, Aziz D. Confocal microscopy through a fiber-optic imaging bundle. Opt Lett. 1993; 18(8):565. [PubMed: 19802201]
78. Kester RT, Tkaczyk TS, Descour MR, Christenson T, Richards-Kortum R. High numerical aperture microendoscope objective for a fiber confocal reflectance microscope. Opt Express. 2007; 15(5):2409–20. [PubMed: 19532478]
79. Zhong W, Celli JP, Rizvi I, Mai Z, Spring BQ, Yun SH, et al. In vivo high-resolution fluorescence microendoscopy for ovarian cancer detection and treatment monitoring. Br J Cancer. 2009; 101(12):2015–22. [PubMed: 19920823]
80. Arridge SR, Lionheart WR. Nonuniqueness in diffusion-based optical tomography. Opt Lett. 1998; 23(11):882–4. Epub 2007/12/19. [PubMed: 18087373]
81. Dunn A, Boas D. Transport-based image reconstruction in turbid media with small source-detector separations. Opt Lett. 2000; 25(24):1777–9. Epub 2007/12/11. [PubMed: 18066341]
82. Hillman EM, Boas DA, Dale AM, Dunn AK. Laminar optical tomography: demonstration of millimeter-scale depth-resolved imaging in turbid media. Opt Lett. 2004; 29(14):1650–2. Epub 2004/08/18. [PubMed: 15309848]
83. Konecky S, Mazhar A, Cuccia D, Durkin A, Schotland J, Tromberg B. Quantitative optical tomography of sub-surface heterogeneities using spatially modulated structured light. Opt Express. 2009; 17(17):14780–90. [PubMed: 19687956]
84. Zhang X, Badea C, Johnson G. Three-dimensional reconstruction in free-space whole-body fluorescence tomography of mice using optically reconstructed surface and atlas anatomy. J Biomed Opt. 2009; 14(6):064010. [PubMed: 20059248]
85. Balas C. Review of biomedical optical imaging-a powerful, non-invasive, non-ionizing technology for improving in vivo diagnosis. Measurement Science & Technology. 2009; 20(10)
86. Kirsch DG, Dinulescu DM, Miller JB, Grimm J, Santiago PM, Young NP, et al. A spatially and temporally restricted mouse model of soft tissue sarcoma. Nature Medicine. 2007; 13(8):992–7.
87. Skliarenko JV, Lunt SJ, Gordon ML, Vitkin A, Milosevic M, Hill RP. Effects of the vascular disrupting agent ZD6126 on interstitial fluid pressure and cell survival in tumors. Cancer Res. 2006; 66(4):2074–80. Epub 2006/02/21. [PubMed: 16489007]
88. Standish BA, Yang VX, Munce NR, Wong Kee Song LM, Gardiner G, Lin A, et al. Doppler optical coherence tomography monitoring of microvascular tissue response during photodynamic therapy in an animal model of Barrett's esophagus. Gastrointest Endosc. 2007; 66(2):326–33. Epub 2007/07/24. [PubMed: 17643708]
89. Joo C, Evans CL, Stepinac T, Hasan T, de Boer JF. Diffusive and directional intracellular dynamics measured by field-based dynamic light scattering. Opt Express. 2010; 18(3):2858–71. Epub 2010/02/23. [PubMed: 20174115]
90. Skala MC, Fontanella A, Lan L, Izatt JA, Dewhirst MW. Longitudinal optical imaging of tumor metabolism and hemodynamics. J Biomed Opt. 2010; 15(1):011112. Epub 2010/03/10. [PubMed: 20210438]
91. Skala M, Fontanella A, Lan L, Izatt J, Dewhirst M. Longitudinal optical imaging of tumor metabolism and hemodynamics. J Biomed Opt. 2010; 15(1):011112. [PubMed: 20210438]
92. Favazza, C.; Wang, L. In Vivo Photoacoustic Tomography. In: Tunnell, J., editor. In Vivo Clinical Imaging and Diagnosis. McGraw Hill; New York, NY: 2011. p. 127-59.
93. Hu S, Wang LV. Neurovascular photoacoustic tomography. Front Neuroenergetics. 2010; 2:10. Epub 2010/07/10. [PubMed: 20616885]

94. Hu S, Wang LV. Photoacoustic imaging and characterization of the microvasculature. J Biomed Opt. 2010; 15(1):011101. Epub 2010/03/10. [PubMed: 20210427]

95. Wang LV. Prospects of photoacoustic tomography. Med Phys. 2008; 35(12):5758–67. Epub 2009/01/30. [PubMed: 19175133]

96. Hu S, Maslov K, Wang LV. In vivo functional chronic imaging of a small animal model using optical-resolution photoacoustic microscopy. Med Phys. 2009; 36(6):2320–3. Epub 2009/07/21. [PubMed: 19610320]

97. Li C, Wang LV. Photoacoustic tomography and sensing in biomedicine. Phys Med Biol. 2009; 54(19):R59–97. Epub 2009/09/03. [PubMed: 19724102]

98. Kim C, Favazza C, Wang LV. In vivo photoacoustic tomography of chemicals: high-resolution functional and molecular optical imaging at new depths. Chem Rev. 2010; 110(5):2756–82. Epub 2010/03/10. [PubMed: 20210338]

99. Yuan Z, Jiang H. Photoacoustic tomography for imaging nanoparticles. Methods Mol Biol. 2010; 624:309–24. Epub 2010/03/11. [PubMed: 20217605]

100. Zhang Q, Iwakuma N, Sharma P, Moudgil BM, Wu C, McNeill J, et al. Gold nanoparticles as a contrast agent for in vivo tumor imaging with photoacoustic tomography. Nanotechnology. 2009; 20(39):395102. Epub 2009/09/04. [PubMed: 19726840]

101. Liang F, Chen B. A review on biomedical applications of single-walled carbon nanotubes. Curr Med Chem. 2010; 17(1):10–24. Epub 2009/11/28. [PubMed: 19941481]

102. Oladipupo SS, Hu S, Santeford AC, Yao J, Kovalski JR, Shohet RV, et al. Conditional HIF-1 induction produces multistage neovascularization with stage-specific sensitivity to VEGFR inhibitors and myeloid cell independence. Blood. 2011; 117(15):4142–53. Epub 2011/02/11. [PubMed: 21307392]

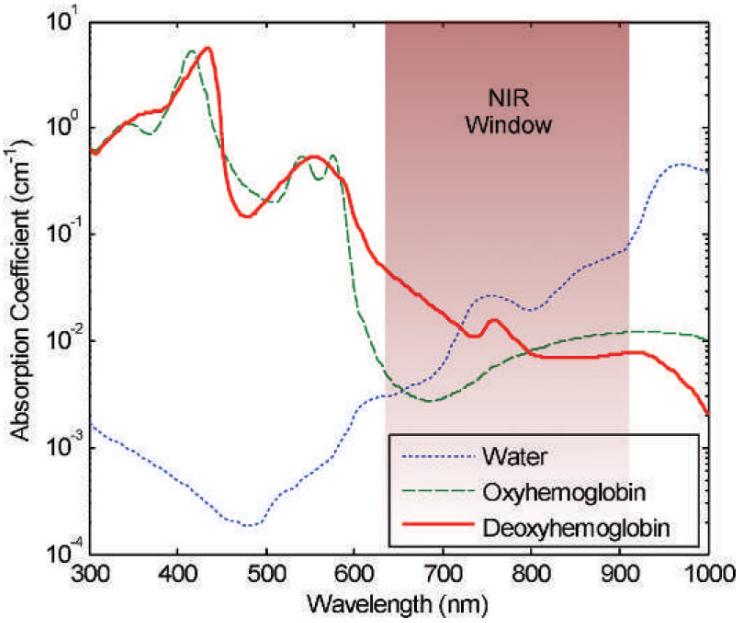


**FIG. 1.**

The NIR window has relatively low absorption, enabling deeper penetration of light. Absorption is shown for 10 μ*M* hemoglobin (22) and water (23). (Reproduced with permission from ref. 24.)

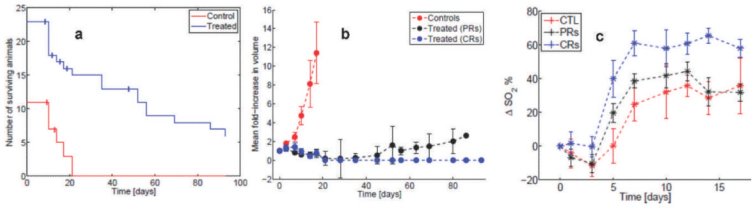


**FIG. 2.**

Panel a: Shows the number of surviving animals in time (censored animals are indicated by the vertical ticks at the points of censoring); blue line: treated group; red line: control group. Panel b shows the mean fold-increase in tumor volume for the treated (black and blue curves) and untreated animals (controls, red curve). The treated animals were classified as those achieving local control (complete responders, CRs: blue line) or local recurrence (partial responders, PRS: black line) based on the presence or absence of tumor 90 days post-treatment. Panel c shows the average change in tumor hemoglobin saturation (relative to day 0, $\Delta SO_2$) for each group (blue curve: CRs; black curve: PRs; red curve: controls). (Reproduced from ref. 57.)

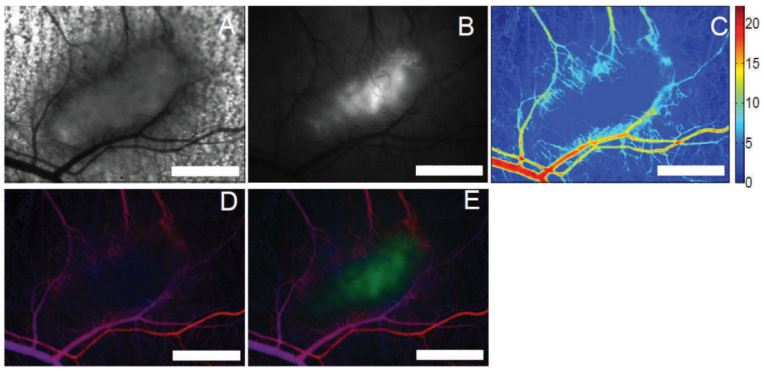


**FIG. 3.**

Examples of functional data obtainable by intravital microscopy including the (panel A) bright field transmission image. Panel B: HIF-1 GFP reporter fluorescence (32), (panel C) total hemoglobin content, (panel D) hemoglobin oxygen saturation on a red-blue color scale (red: well oxygenated, blue: poorly oxygenated) whose brightness is modulated by the total hemoglobin content (making vessels appear bright), and (panel E) an overlay view of panels D and B with the GFP channel appearing in green. The tumor appears as the pickle-shaped object in the center of the view. The edge of the tumor can be seen to be highly-vascularized, with relatively few vessels in the hypoxic center of the tumor. Scale bars are 1 mm. (Reproduced with permission from ref. 63.)

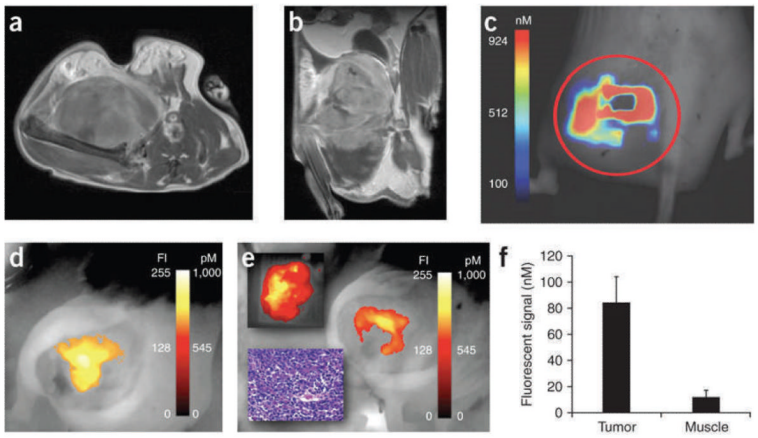


**FIG. 4.**

Axial (panel a) and coronal (panel b) images of gadolineum-DTPA enhanced T1 MRI images show the sarcoma tumor and surrounding tissue of the gluteal region. The corresponding FMT image (panel c) was taken after injection of a Prosense probe, an NIR fluorescent protease-activated probe (VisEn Medical, Inc.). Finally, a hand-held imaging system was used to acquire Prosense fluorescence prior to (panel d) and after (panel e) surgical resection of the tumor. After surgery (panel e), the resected tumor show fluorescence (upper inset), while pathology confirms tumor tissue (lower inset), and some residual tumor remains in the surgical cavity (primary panel e). Finally, the specificity of the probe for tumor tissue was verified using FMT to compare the tumor and contralateral normal muscle tissue fluorophore concentration. (Reproduced with permission from ref. 86.)

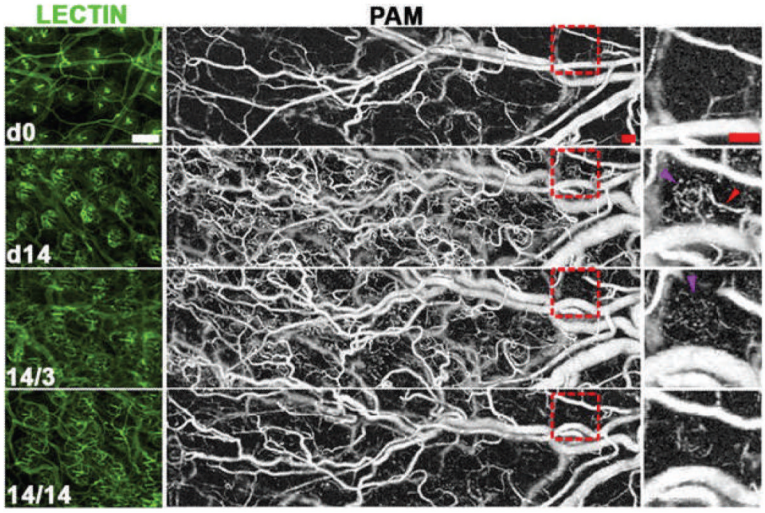


**FIG. 5.**

Lectin-perfused whole mounts (left column) and PAM images (middle column) with a magnified view of the boxed region shown in the right column. Images were acquired at day 0 (d0) and day 14 (d14) of HIF induction followed by withdrawal of HIF-1 induction for 3 and 14 days (14/3: 14 days on, 3 days off; 14/14: 14 days on, 14 days off). This demonstrates the ability of PAM to monitor vascular morphology longitudinally in the same animal, and enables quantification of the induction of angiogenesis followed by selective vascular regression after removal of HIF-1 induction. Purple arrows indicate a perifollicular neocapillary unit detected by PAM with the adjacent vascular supply arch indicated by the red arrow. Scale bars represent 100 μm. (Reproduced with permission from (102).)

## TABLE 1

Sources of Optical Contrast Available for Optical Imaging and Spectroscopy

| Optical process | Sources of contrast | Functional/morphological relevance |
|---|---|---|
| 1. Tissue absorption (12–14) | Hemoglobin/myoglobin | Hemoglobin/myoglobin concentration and oxygen saturation |
| | Melanin | Melanin concentration |
| | Carotene | Carotene concentration (adipose tissue content) |
| | Protein/DNA other UV absorbers | Cellular density, tissue morphology |
| 2. Tissue scattering (12, 13) | Local inhomogeneity including cell organelles, extracellular matrix, and membranes | Tissue morphology |
| 3. Tissue fluorescence (13, 14) | NADH and FAD | Cellular redox state |
| | Collagen/elastin | Tissue morphology |
| | Tryptophan | Protein or cellular density and morphology |
| | Porphyrins | Heme synthesis and porphyrin accumulation |
| 4. Extrinsic absorption | Small molecular chromophores | Biodistribution of a given chromophore, which may be targeted or untargeted, and can reflect a wide range of functional indicators |
| | Nanoparticle absorption | Biodistribution of an absorbing nanoparticle, which could include nanospheres, nanoshells, and carbon nanotubes. May be targeted or untargeted |
| 5. Extrinsic scattering | Nanoparticle scatterers | Scattering nanoparticles include nanospheres, nanoshells, and carbon nanotubes. May be targeted or untargeted |
| 6. Extrinsic fluorescence | Small molecular fluorophores | Can be activatable, targeted, or untargeted, and can report on many parameters such as pH, hypoxia, gene expression, ion concentration and membrane potential |
| | Nanoparticle fluorescence | Biodistribution of a nanoparticle that may be intrinsically fluorescent or loaded with a fluorescent molecule |
| 7. Luminescence | Bioluminescent reporters or nanoparticles | Luciferase transfection into transgenic animal or cell line |

## TABLE 2

Summary of the Optical Methods Reviewed in this Manuscript, Including Their Approximate Typical Resolutions, Sensing Depths, and Available Sources of Contrast (Cross References to Categories Listed in Table 1)

| Method | Lateral spatial resolution | Sensing depth | Source(s) of contrast |
|---|---|---|---|
| Fiber-based optical spectroscopy | Point measurements or coarse scanning (>1 mm) (12) | ~0.1–10 mm, depending on probe geometry and wavelength | 1, 2, 3, 4, 5, and 6 |
| Optical coherence tomography (OCT) | 4–20 microns (15) | 1 mm | 2 and 5 primarily, possible to do 1 and 4 |
| Photoacoustic tomography (PAT)/ photoacoustic microscopy (PAM) | 45 μm to 1 mm (scalable with depth) (16) | Several cm (16) | 1 and 4 |
| Diffuse optical tomography (DOT) | mm to cm (17) | Several cm (17) | 1, 2, 4, and 5 |
| Fluorescence molecular tomography (FMT) | Sub-mm to cm (18, 19) | Several cm (18, 19) | Primarily 6, also 3 |
| Intravital microscopy and microendoscopy | 200 nm (15) | Several hundred microns (19, 20) | 1, 2, 3, 4, 5, and 6 |